Cell Reports
Article

Hyperacidification of Vacuoles by the Combined Action of Two Different P-ATPases in the Tonoplast Determines Flower Color

Marianna Faraco,[1,6,7] Cornelis Spelt,[1,6] Mattijs Bliek,[1] Walter Verweij,[1,8] Atsushi Hoshino,[1,2,3] Luca Espen,[4] Bhakti Prinsi,[4] Rinse Jaarsma,[1] Eray Tarhan,[1] Albertus H. de Boer,[1] Gian-Pietro Di Sansebastiano,[5] Ronald Koes,[1,*] and Francesca M. Quattrocchio[1,*]

[1]Department of Molecular Cell Biology, Graduate School of Experimental Plant Sciences, VU University, De Boelelaan 1085, 1081HV Amsterdam, the Netherlands
[2]National Institute for Basic Biology, Nishigonaka 38, Myodaiji, Okazaki, 444-8585 Aichi, Japan
[3]Department of Basic Biology, The Graduate University for Advanced Studies (Sokendai), 444-8585 Okazaki, Japan
[4]Dipartimento Scienze Agrarie e Ambientali, Produzione, Territorio, Agroenergia, Università degli Studi di Milano, Via G. Celoria 2, 20133 Milano, Italy
[5]Di.S.Te.B.A., Università del Salento, Campus Ecotekne, 73100 Lecce, Italy
[6]These authors equally contributed to this work
[7]Present address: Di.S.Te.B.A., Università del Salento, Campus Ecotekne, 73100 Lecce, Italy
[8]Present address: The Genome Analysis Centre, Norwich Research Park, Colney, Norwich, NR4 7UH, UK
*Correspondence: ronald.koes@vu.nl (R.K.), f.m.quattrocchio@vu.nl (F.M.Q.)
http://dx.doi.org/10.1016/j.celrep.2013.12.009

SUMMARY

The acidification of endomembrane compartments is essential for enzyme activities, sorting, trafficking, and *trans*-membrane transport of various compounds. Vacuoles are mildly acidic in most plant cells because of the action of V-ATPase and/or pyrophosphatase proton pumps but are hyperacidified in specific cells by mechanisms that remained unclear. Here, we show that the blue petal color of petunia ph mutants is due to a failure to hyperacidify vacuoles. We report that PH1 encodes a P_{3B}-ATPase, hitherto known as $Mg2^+$ transporters in bacteria only, that resides in the vacuolar membrane (tonoplast). In vivo nuclear magnetic resonance and genetic data show that PH1 is required and, together with the tonoplast H^+ P_{3A}-ATPase PH5, sufficient to hyperacidify vacuoles. PH1 has no H^+ transport activity on its own but can physically interact with PH5 and boost PH5 H^+ transport activity. Hence, the hyperacidification of vacuoles in petals, and possibly other tissues, relies on a heteromeric P-ATPase pump.

INTRODUCTION

The pH within cellular compartments controls enzymatic reactions, protein sorting, vesicular traffic, and stability of metabolites in their lumen and relies on the activity of transporters that translocate protons and other ions across membranes (Casey et al., 2010). Vacuoles are the largest endomembrane compartment in plant cells, occupying up to 90% of the cell volume. They act as lytic compartments and/or as reservoirs of ions and other molecules and are involved in building of turgor and the detoxification of metabolites and xenobiotics (Marty, 1999). In most plant cells, the cytoplasm is about neutral and the lumen of the vacuole is mildly acid (pH_{vac} ~6), whereas vacuoles can be more acidic (hyperacidified) in specialized tissues, like epidermal cells of petunia petals (pH_{vac} ≤5; see below) or juice cells in lemons (pH_{vac} <3).

Endomembrane compartments are acidified by V-ATPase proton pumps, which translocate H^+ from the cytoplasm into their lumen (Casey et al., 2010; Gaxiola et al., 2007). The membrane surrounding vacuoles (tonoplast) of plant cells contains in addition a pyrophosphatase proton pump (Gaxiola et al., 2007; Maeshima, 2001). H^+ pumping is electrogenic and produces an electrochemical gradient ($\Delta\mu^{H+}$) consisting of an electrical potential ($\Delta\psi$) and a chemical concentration difference (ΔpH) that quickly inhibits further (bulk) proton import (Casey et al., 2010; Mindell, 2012; Sze, 1985). Hence, $\Delta\psi$ needs to be dissipated, for example, by anion transporters that mediate an anion influx or a cation efflux from the vacuole, to enable massive proton import. Lysosomes of animal cells need a Cl^-/H^+ antiporter to reduce $\Delta\psi$ for massive proton import and acidification of the lumen (Graves et al., 2008). It is likely that the acidification of plant vacuoles, in particular, those with low pH, depends on ion transporters (Barbier-Brygoo et al., 2011), which can dissipate $\Delta\psi$, and perhaps additional transporters or regulators that maintain low pH. In theory, V-ATPases, together with other transporters, can generate a pH gradient of 3 (Rea and Sanders, 1987); however, the establishment and maintenance of steep pH gradients, as in (very) acid

vacuoles of special cell types, may need additional regulatory components.

The coloration of most flowers and fruits is controlled by a widely conserved complex of MYB, HLH, and WD40 transcription regulators, known in petunia as ANTHOCYANIN2 (AN2), AN1, and AN11, which activate some 15 genes encoding enzymes involved in anthocyanin synthesis (Koes et al., 2005) and, at least in corn, their transport to the vacuole (Goodman et al., 2004). The hue of the tissue depends on factors that shift the anthocyanin absorption spectrum, such as, the presence of copigments (e.g., flavonols), metals ions, and the pH inside the vacuole (Koes et al., 2005; Yoshida et al., 2009). In *Ipomoea*, for example, the petal color changes from purple to blue upon opening of the flower, which is due to alkalinization of the vacuole by a Na^+/H^+ and K^+/H^+ exchanger (NHX) in the tonoplast that is encoded by *PURPLE* (Fukada-Tanaka et al., 2000; Yoshida et al., 1995). Petunia flowers normally have a red or violet color and mutations in seven loci, named *PH1–PH7*, result in a bluish color (de Vlaming et al., 1983; van Houwelingen et al., 1999). Because these mutations reduced the acidity of crude petals homogenates, the color change was thought to result from reduced acidity of vacuoles rather than altered metal ion content (de Vlaming et al., 1983).

Molecular analysis showed that PH5 belongs to the 3A family of P-ATPases (Verweij et al., 2008). P-ATPases constitute a superfamily of ATP-powered membrane transporters, grouped in ten phylogenetic clades of pumps that translocate distinct cations (Palmgren and Nissen, 2011). The 3A subfamily (P_{3A}-ATPases) of plants, fungi, and other unicellular eukaryotes comprises proton pumps that reside in the plasma membrane, control cytoplasmic pH, and energize the transport of ions and organic compounds via other transporters. PH5, however, resides in the tonoplast, suggesting that it operates in a pathway that acidifies the vacuole (Verweij et al., 2008). PH3 and PH4 are transcription factors that together with AN1, also known as PH6 (Spelt et al., 2002), and AN11, activate expression of *PH5* and at least ten more genes of unknown function (Verweij, 2007; Verweij et al., 2008). Therefore, the blue color of *ph3*, *ph4*, and *an1*/*ph6* petals is at least in part due to reduced *PH5* expression. However, enforced expression of PH5 in transgenic plants did not rectify the *ph3* and *ph4* petal color phenotype, suggesting that besides PH5 other (unknown) factors are required for bulk proton transport into the vacuole (Verweij et al., 2008).

Here, we report that *PH1* is a target gene of PH3, PH4, AN1, and AN11 and that it encodes a P-ATPase of the 3B family, previously believed to comprise bacterial Mg^{2+} transporters only (Kühlbrandt, 2004). We provide direct evidence that *ph1*, *ph3*, *ph4*, and *ph5* mutations reduce the acidification of the vacuoles and that coexpression of PH1 and PH5 is sufficient to restore hyperacidification of vacuoles in petals of regulatory mutants (*ph3*, *ph4*) and to acidify vacuoles in leaves, where these genes are otherwise not expressed. PH1 can interact directly with PH5 and boost its proton pumping activity, indicating that PH1 and PH5 constitute a heteromeric proton transporter operating in cells where hyperacidification of the vacuole is required for specific functions.

RESULTS

Isolation of *PH1*

To obtain transposon-tagged *ph1* alleles, we crossed a stable *ph1* line (R67) to a $PH1^+$ line (W138) containing active *dTPH1* transposons. The off-spring consisted of ~7,000 plants with red-colored flowers, as expected for $PH1^{+/-}$ petals synthesizing red-colored anthocyanins (cyanidins), and one unstable mutant (plant L2164-1) having purplish petals with occasional red spots and sectors, as expected for an unstable transposon-tagged *ph1* mutant (Figure 1A). The petal color of this (*ph1*) mutant is similar to that of a *ph5* mutant in a cyanidin background. However, unlike *ph5*, the mutation did not abolish the accumulation of brown-colored proanthocyanidins in the seed coat (Figure 1A). The cross of L2164-1 to the *ph1* line V23, which synthesizes fully substituted violet anthocyanins (malvidins), resulted in progeny with either evenly colored blue flowers (*ph1*) or blue flowers with red-violet revertant spots (unstable *ph1*) (Figure 1B), confirming that L2164-1 harbored a unstable *ph1* allele, designated $ph1^{L2164}$.

Analysis of the previously identified PH3/PH4-regulated genes showed that the original $ph1^{L2164/-}$ mutant contained a *dTPH1* insertion in the gene encoding *cDNA-AFLP CLONE7.5* (*CAC7.5*), whereas this insertion was absent from the parents of the mutant and $PH1^{+/-}$ siblings. In two germinal revertant alleles ($PH1^{R1}$ and $PH1^{R2}$), identified in crosses of L2164-1 to line R67, *dTPH1* had excised and created a 6 bp footprint that restored the CAC7.5 reading frame, whereas the insertion was maintained in mutant siblings (Figure 1C). The *ph1* lines R67, V23, V42, and V48 also contain mutated *cac7.5* alleles with either a 7 or 8 bp insertion in the *CAC7.5* coding sequence (Figure 1C). Because these insertions are in the same position and resemble transposon footprints, we assume that they originate from a transposon insertion allele that arose well before 1954 when inbreeding of these lines started. Finally, expression of CAC7.5 from the *35S* promoter in a homozygous $ph1^{V23}$ mutant restored the $PH1^+$ flower color phenotype (Figure 1D). Hence, we concluded that *CAC7.5* is encoded by *PH1*.

PH1 Is Directly Activated by the AN1-PH4-PH3-AN11 Complex

RT-PCR analysis showed that *PH1* is coexpressed with *PH5* in the petal limb and tube, peaking slightly later than anthocyanin genes (*DIHYDROFLAVONOL REDUCTASE*, *DFR*) when the flower bud opens, but not in anthers, which synthesize anthocyanins and express *DFR*, or sepals, leaves, stems, and roots (Figure 2A). Expression of *PH1* mRNA in petals requires the transcription factors PH3, PH4, AN1, and AN11, but was not affected by mutations in *PH2* or *PH5* and the resulting shift in vacuolar pH (Figure 2B). The 8 bp insertion in $ph1^{V23}$ does not abolish the encoded mRNAs as the $ph1^{V23}$ petals expressed a normal amount of (mutated) *PH1* transcripts. Similarly, the transposon insertions in $ph5^{R159}$ and/or $ph5^{V69}$ alleles do not abolish the (nonfunctional) *ph5* transcripts in $ph5^{V69/R159}$ petals. *PH1* is, like *PH5* and *DFR*, expressed in young (virgin) buds in the ovaries. Some 15 days after pollination, *PH1* and *PH5* expression is upregulated together with *DFR* and proanthocyanidin synthesis in seeds, in an AN1-dependent manner (Figure 2C).

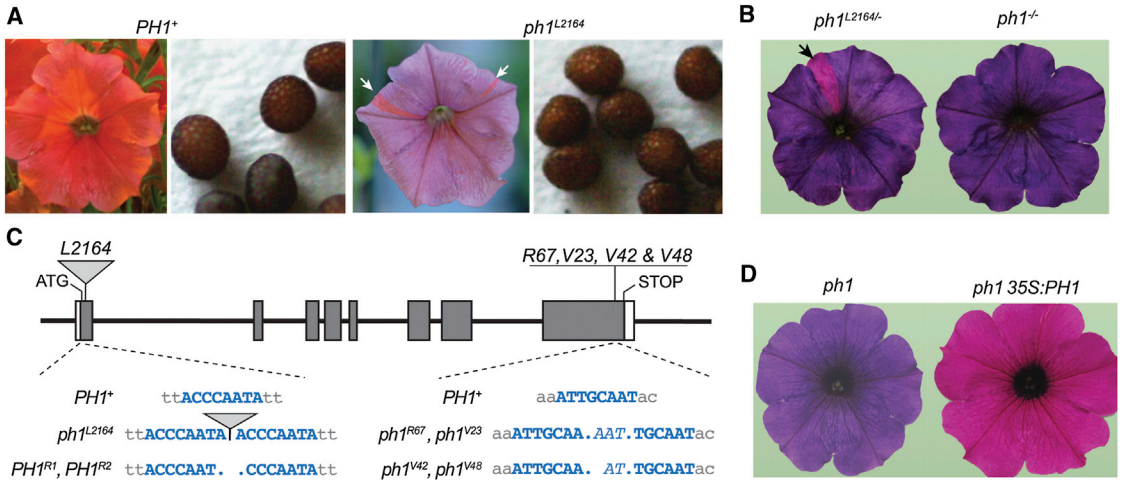

Figure 1. Isolation of *PH1*

(A) Flowers and seeds of a PH1$^{+/-}$ plant and an unstable mutant (*ph1*$^{L2164/-}$) obtained by a cross of lines R67 (*ph1*$^{-/-}$) × W138 (*PH1*$^{+/+}$). Anthocyanins in this background are cyanidins.

(B) F_1 progeny of the tagged mutant (*ph1*$^{L2164/-}$) from (A) and line V23 (*ph1*$^{-/-}$) with an unstable (left) and stable recessive *ph1* phenotype. Anthocyanins in this background are malvidins. Revertant sectors in (A) and (B) are indicated by arrows.

(C) Diagram of *PH1* and *ph1* alleles. Uppercase blue letter denotes the (putative) target site duplication; dots and italics, nucleotides deleted or inserted after transposon excision.

(D) *ph1* and *ph1 35S:PH1* flower. Anthocyanins in this background (V23 × V30) are malvidin and petunidin.

PH4 and PH3 are MYB and WRKY proteins that interact with the transcription regulators AN1 and AN11 (Quattrocchio et al., 2006; Verweij, 2007). To assess whether this complex activates *PH1* directly, we used an *an1* line expressing a fusion of AN1 and the ligand-binding domain of the glucocorticoid receptor (GR) from a transgene (*35S:AN1-GR*). Upon exposure to dexamethasone, AN1-GR is posttranslationally activated, and expression of *DFR*, *PH5*, and *PH1* is restored (Spelt et al., 2000) (Figure 2D). Inhibition of protein synthesis with cycloheximide did not block dexamethasone-induced transcription of *DFR*, *PH5* (Spelt et al., 2000; Verweij et al., 2008), or *PH1* in the first 2 hr (Figure 2D), indicating that AN1 activates *DFR*, *PH5*, and *PH1* expression directly. After 20 hr, the *DFR*, *PH5*, and *PH1* mRNA levels drop again, which is due to the turnover of the AN1-GR protein (Spelt et al., 2000). These data show that *PH1* has a spatiotemporal expression pattern very similar to that of *PH5* and is (directly) activated by the same transcription regulators.

PH1 Is Highly Similar to Prokaryotic P_{3B}-ATPases

PH1 displays high similarity to P_{3B}-ATPases (Figure S1A), which were identified for their capacity to mediate Mg^{2+} uptake in bacteria (Maguire, 2006), but were thought to be absent from plants, fungi, and animals (Pedersen et al., 2012; Thever and Saier, 2009). Analysis of the membrane topology of MgtB from Salmonella suggested a structure consisting of ten *trans*-membrane domains and C- and N-terminal domains residing in the cytosol (Smith et al., 1993). The similarity of PH1 with MgtA and MgtB suggests the same structure implying that PH1 can translocate cations in the same direction, which is from the "outside" (vacuolar lumen or periplasmic space) into the cytosol (Figure S1B).

Database searches identified proteins from several Angiosperms with high similarity to PH1 (Figure S2). Phylogenetic analysis showed that these plant proteins group with bacterial P_{3B}-ATPases in a clade only distantly related to the H^+ P_{3A}-ATPases (Figure 3), in line with the entirely different intron/exon architecture of P_{3A}- and P_{3B}-ATPase genes (Figure 1C) (Verweij et al., 2008). However, the proteins of rice (Os03 g0616400) and *Arabidopsis* (At ACA2) with the highest similarity to PH1 belong to different P-ATPase subfamilies, indicating that PH1 homologs or other P_{3B}-ATPases are lacking in these species (Figure 3).

Subcellular Localization of PH1

To study the localization of PH1 in petal cells, we generated *ph1* plants expressing PH1-GFP fusion proteins. Transgenes expressing PH1 with a GFP-tag on either the N or C terminus (*35S:GFP-PH1* and *35S:PH1-GFP*) efficiently rescued the flower color and the petal extract pH of the *ph1* mutant (Figures S3A–S3C). Nevertheless, we could not detect any GFP-fluorescence or proteins cross-reacting with GFP antibodies in *35S:PH1-GFP* tissues, whereas in *35S:GFP-PH1* tissues we observed only a truncated protein of ~30 kDa that accumulated in a highly variable punctate pattern in epidermal petal cells (Figures S3C–S3E). Next, we tested a PH1 fusion in which GFP was inserted in the first predicted cytoplasmic loop of PH1 (PH1-GFPi, GFP-internal). Expression of *35S:PH1-GFPi* hardly rescued the *ph1* phenotype but resulted in the accumulation of a full size (~130 kDa) fusion protein, making it a reliable marker for PH1 localization (Figures 4A–4C). PH1-GFPi accumulates in petals at a much lower level than PH5-GFP possibly due to low protein stability, which explains the poor rescue of the *ph1* defect. Transient expression in petal protoplasts, which faithfully reproduce the sorting of proteins in the intact tissue (Faraco et al., 2011), showed that most PH1-GFPi resides in a membrane that is internal to and distinct from the plasma membrane

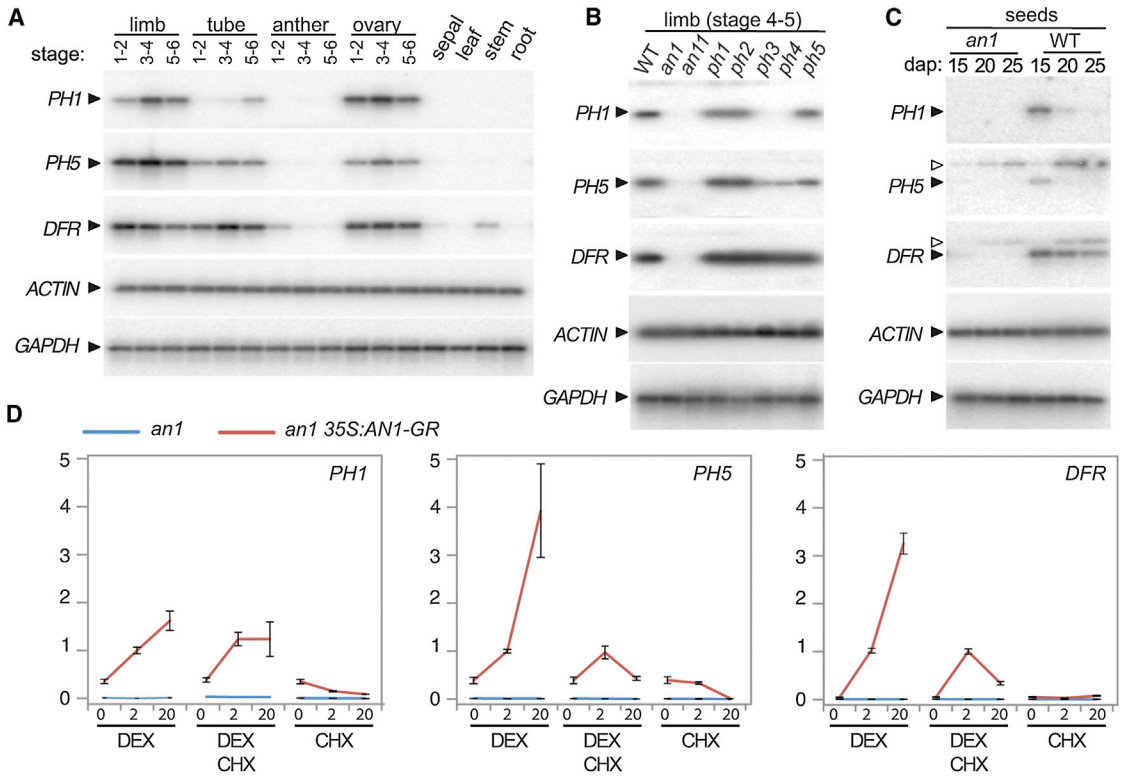

Figure 2. Expression Pattern and Genetic Regulation of *PH1*

(A–C) RT-PCR analysis of developing flowers and vegetative tissues of the wild-type line R27 (A), petals of R27 and isogenic mutants (B), and seeds of R27 (AN1^{+}) and an isogenic *an1* line (C).

(D) Real-time PCR analysis of *PH1*, *PH5*, and *DFR* mRNA in the petal limbs of stage 4 *an1 35S:AN1-GR* buds and, as a control, *an1* mutants after 2 or 20 hr of exposure to dexamethasone (DEX) and/or cycloheximide (CHX). Stages 1–2, young buds; 3–4, (near) full-length buds; 5–6, opening and fully opened flowers. Dap, days after pollination.

marked by RFP-AtSYP122 (Assaad et al., 2004) (Figures 4D–4F). The same localization was observed in colored cells from the epidermis, where *PH* genes are expressed (Quattrocchio et al., 2006; Verweij et al., 2008), and white mesophyll cells that lack expression of *PH* genes. We cannot exclude that some of the PH1-GFPi fluorescence originates from small compartments, like vesicles or prevacuoles, in the cytoplasm.

Constitutive Coexpression of PH1 and PH5 Rescues the *ph3* Mutant and Acidifies Leaves

Petunia flowers accumulating cyanidin derivatives have a red color, and the pH of petal extracts is around 5.5 if all *PH* genes are functional. In this background, the *ph3* mutation results in bluish/grayish petals in which crude extract has a pH around 6 (Figures 5A and 5B). As *PH1* is a PH3-regulated gene, we asked whether expression of PH1 together with PH5 is sufficient to rectify the *ph3* phenotype.

Constitutive expression of PH5 (*35S:PH5*) did not rectify the phenotype of *ph3* petals (Verweij et al., 2008). Likewise, a *35S:PH1* transgene complemented the *ph1* mutation efficiently (Figure 1C) but not *ph3* even though the transgene was sufficiently expressed (Figures 5A–5C). Introduction of *35S:PH1* in *ph3 35S:PH5* plants, however, rectified both the *ph3* petal color and pH of petal extracts (Figures 5A and 5B). Constitutive coexpression of PH1 and PH5 also rectified the pH of *an1* petal homogenates (Figure 5B), but not the synthesis of anthocyanins, as expected. In a *ph4* background *35S:PH1* and *35S:PH5* decreased the petal extract pH, but not enough to restore the normal flower color, possibly due to insufficiently high expression of (one of) the transgenes (Figure 5C). Constitutive coexpression of *PH1* and *PH5* also reduced the pH of leaf homogenates (Figure 5B). These findings indicate that *PH1* and *PH5* are the primary AN1-PH3-PH4 target genes that acidify vacuoles in epidermal petal cells and are sufficient to lower the pH in vacuoles also in tissues where they are normally not expressed.

PH1, PH3, and PH5 Affect Petal Color via Acidification of Vacuoles

Although the petal color and pH of the petal homogenates in mutants is suggestive, direct evidence that *PH* genes promote vacuolar acidification is lacking. To directly examine vacuolar pH, we subjected petal and leaf fragments of different genotypes to in vivo ^{31}P-NMR spectroscopy (Roberts, 1987). In ^{31}P-NMR spectra of living tissues, the main peak originates from vacuolar phosphate (Pi_{vac}) (Figure S4A), and we inferred the average vacuolar pH from the Pi_{vac} chemical shift (δ) using a titration curve (Figures S4B–S4D). The vacuolar pH is increased in *an1* petals compared to isogenic *AN1*$^{+}$ petals, and also in *ph1* and

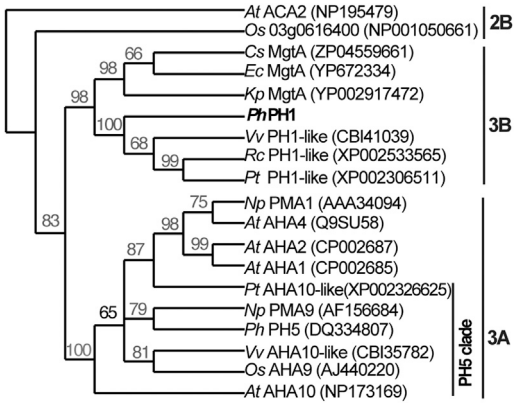

Figure 3. Cladogram of PH1 Homologs from Different Species

The tree is based on alignments of full proteins from petunia (*Ph*), *Arabidopsis* (*At*), Citrobacter (*Cs*), *E. coli* (*Ec*), grape (*Vv*), Klebsiella (*Kp*), N. plumbaginifolia (*Np*), Populus (*Pt*), rice (*Os*), and Ricinus (*Rc*). The accession numbers is given for each protein. Bold letters and numbers on the right indicate P-ATPase subfamilies. PH1 homologs cluster with bacterial Mg^{2+} transporters of the 3B family. Note that proteins from grape (VvPH1-like) Ricinus (Rh-PH1-like) and Populus (Pt-PH1 like) with most similarity to PH1 form a clade of (plant) P_{3B} ATPases, whereas those from rice (Os03 g0616400) and *Arabidopsis* (At ACA2) belong to a different subfamily. See also Figures S1 and S2.

ph5 petals when compared to transgenic siblings expressing PH1 or the grape PH5 homolog (VvAHA10-like) (Figure 6). The ectopic coexpression of PH1 and PH5 also reduced vacuolar pH in leaves, whereas either PH1 or PH5 alone had little or no effect (Figure 6), consistent with the pH values of crude leaf extracts (Figure 5B). Curiously, the PH5 homolog from grape (VvAHA10-like) also reduced vacuolar pH in leaves, which may indicate that VvAHA10-like is more active in the absence of PH1 than petunia PH5.

To examine directly whether the altered petal color of *ph* mutants is (entirely) due to reduced vacuolar acidity, or involves defects in other processes, we generated transgenic plants expressing a vacuolar Na^+/H^+ and K^+/H^+ antiporter (NHX). Expression of NHX proteins was shown to reduce vacuolar acidity in *Ipomoea* flowers (Yoshida et al., 1995), and *Arabidopsis* roots (Bassil et al., 2011). Expression of a petunia *NHX* gene (Yamaguchi et al., 2001) from the *35S* promoter in the red-flowering *ph3* *35S:PH1* *35S:PH5* line eradicated the effect of PH1 and PH5 expression and reinstated the purplish petal color and the pH values of petal and leaf extracts of the *ph3* host (Figures 5A and 5B). This confirms that *PH* genes alter vacuolar pH, like *NHX*, though in the opposite way, and demonstrates that the altered color and petal extract pH is caused by reduced acidity of the vacuole.

Activity of PH1 in *E. coli* and Yeast

PH5 and plasma membrane P_{3A}-ATPases, such as NpPMA4 from *Nicotiana plumbaginifolia*, are able to restore the growth in acidic media of a yeast mutant (YAK2) lacking plasma membrane H^+-ATPases (Verweij et al., 2008) (Figure S5). Expression of the full-size PH1 protein or derivatives lacking 22 amino acids at the N terminus (PH1-ΔN) or ten at the C terminus (PH1-ΔC), which might act as autoinhibitory domains (Palmgren and Nissen, 2011), could not restore growth of YAK2 in acid media, suggesting that PH1 cannot translocate protons (Figures S5A and S5C). Coexpression of PH1 enhanced the growth of YAK2 cells expressing PH5 only slightly, but not of cells expressing the NpPMA4.

Given that bacterial P_{3B}-ATPases can mediate Mg^{2+} uptake across the cell membrane (Maguire, 2006), PH1 might dissipate the voltage across the tonoplast by Mg^{2+} export to enable bulk proton import by PH5. Because it is difficult to directly measure ion transport across the tonoplast of petal cells, we used genetic assays to examine whether PH1 can transport Mg^{2+}.

We could only clone a contiguous PH1 open reading frame behind the tightly-regulated *RhaT* promoter, not in the multiple cloning sites or behind the *MgtA* promoter in high-copy vectors. However, rhamnose-induction severely inhibited growth/survival of *E. coli*, making it impossible to test whether PH1 can rescue *mgtA* (Figure S5C). In a complementary approach, we expressed MgtA or a MgtA-GFP fusion in petunia *ph1* plants. Although we obtained several transformants expressing *MgtA* or *MgtA-GFP* mRNA, we observed no rescue of the *ph1* petal phenotype (Figure S5D).

Given that PH1 expression was not toxic to yeast, we examined whether PH1 could rescue a yeast strain that lacks the Mg^{2+} transporters ALR1 and ALR2 and fails to grow on low Mg^{2+} concentrations. Growth is rescued by expression of either ALR1 or the *Arabidopsis* Mg^{2+} transporter MGT10, as shown before (Li et al., 2001), but not by expression of PH1 or MgtA (Figure S5E).

These results suggest that PH1 may not transport Mg^{2+}, although other explanations, such as mislocalization of PH1 (and MgtA) or absence of an essential partner protein in the heterologous host, cannot be ruled out.

PH1 Interacts with PH5 and Boost PH5 Activity

We next examined whether PH1 might promote PH5 activity by binding to it. Therefore, we performed bimolecular fluorescence complementation assays (BiFC; split-YFP) with a PH1 fusion containing the C-terminal half of YFP (cYFP) in the first predicted cytoplasmic loop (PH1-cYFPi), and a C-terminal fusion of PH5 with either the N-terminal or C-terminal half of YFP (PH5-nYFP or PH5-cYFP). We observed fluorescence in epidermal petal protoplasts coexpressing PH5-nYFP with either PH5-cYFP or PH1-cYFPi (Figure 7A), whereas fluorescence was never detected in protoplasts transformed with any of these fusions and the empty vector expressing the complementary half of YFP.

We confirmed these results using a split-ubiquitin yeast two-hybrid assay (Obrdlik et al., 2004). Yeast cells coexpressing a fusion of PH5 to the C-terminal ubiquitin moiety (Cub) and fusions of either PH5 or PH1 to the N-terminal moiety (Nub) activated the *HIS*, *ADE*, and *LacZ* reporter genes as good as the positive control, homodimerization of AtKAT1 (Figure 7B). This supports that PH5 can form homodimers, similar to P_{3A}-ATPases in the plasma membrane (Ottmann et al., 2007), as well as a heteromeric complex with PH1.

We measured the activity of PH1 and PH5 by patch clamp of vacuolar membranes. Because it is difficult to use epidermal petal cells for such experiments, we used leaves from transgenic

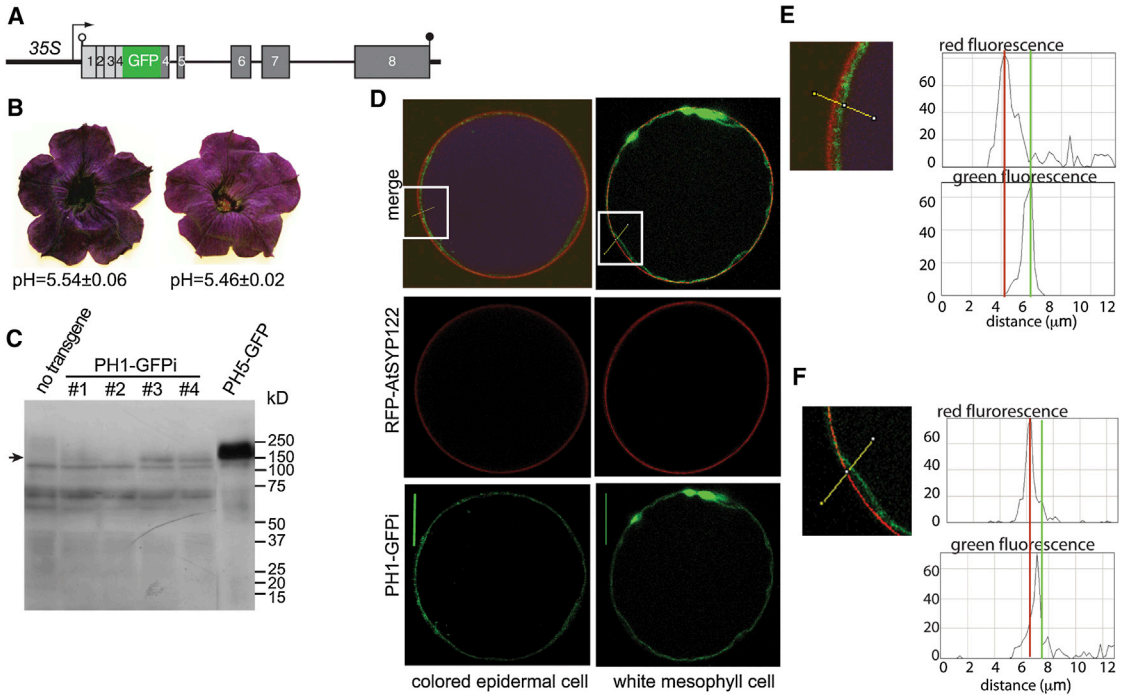

Figure 4. Subcellular Localization of PH1

(A) Diagram of *35S:PH1-GFPi*. The *GFP* cds is inserted in exon 4 between a cDNA (light gray) and genomic *PH1* fragment (dark gray).

(B) Flower phenotype and petal extract pH values of a *ph1* mutant (V30 × V23 background) and a sibling expressing PH1-GFPi with a slightly more reddish color and slightly reduced petal homogenate pH.

(C) GFP fusion proteins detected with anti-GFP in petals of three transformants expressing *35S:PH1-GFPi* (#1, #3 and #4), a sibling that does not express the transgene (#2), a control lacking the transgene, and a *ph5* mutant complemented by a GFP fusion of the rose PH5 homolog.

(D) Confocal image of a petal epidermis protoplast containing anthocyanins, and a petal mesophyll protoplast coexpressing *35S:PH1-GFPi* and the plasma membrane marker RFP-AtSYP12. Fluorescence of anthocyanins is visible in blue, PH1-GFPi in green and RFP-AtSYP122 in red.

(E and F) Distribution of the green (PH1-GFPi) and red (RFP-AtSYP122) fluorescence within the region marked by the white boxes in (D). Note that the green and red signals concentrate on the membranes, whereas hardly any signal is present in the cytoplasm.

Scale bars represent 20 μm. See also Figure S3.

ph3 35S:PH1 and/or *35S:PH5* lines and, as a control, *ph3* leaves. Given that *PH1*, *PH5 PH3*, *AN1*, and *PH4* are not expressed in leaves (Figure 1A) (Quattrocchio et al., 2006; Spelt et al., 2000; Verweij et al., 2008), *ph3* leaves are essentially similar to wild-type (*PH3*$^+$) leaves. In control vacuoles, we measured an ATP-dependent current of about 0.5 pA/pF, that was insensitive to addition of 100 μM vanadate, a specific inhibitor of P-ATPases, (Figures 7C and S6) but strongly inhibited by 40 nM bafilomycin A (Figures 7D and 7E), indicating that it is mediated by a V-ATPase. Vacuoles from *ph3 35S:PH1* leaves behaved similarly, implying that PH1 alone cannot mediate a vanadate-sensitive (proton) current. In contrast, vacuoles from PH5-expressing leaves exhibited a vanadate-sensitive current of around 0.5–1.1 pA/pF (Figure 7C). This indicates that PH5 can transport protons on its own (i.e., in the absence of PH1) and, in addition, confirms that native PH5 resides, like PH5-GFP, in the tonoplast. Coexpression of PH5 and PH1 resulted in a larger vanadate-sensitive current and was associated with a strong reduction of the vanadate-insensitive/bafilomycin-sensitive V-ATPase activity (Figures 7C, 7D, and S5B), indicating that proton translocation in these vacuoles depends for the major part on PH1 and PH5, whereas V-ATPases contribute very little.

These findings suggest that PH1 promotes pumping activity of PH5 and supports the localization of PH1 in the tonoplast. Because the membrane voltage was clamped at 0 mV, the observed upregulation of PH5 activity by PH1 cannot be explained by PH1 mediating a voltage-dissipating ion current, but it is consistent with upregulation of proton pumping activity via the formation of a heteromeric PH5-PH1 complex.

DISCUSSION

All cells maintain a neutral pH in their cytoplasm, whereas the pH in vacuole and therefore the H^+ gradient (ΔpH) across the tonoplast can vary considerably between cell types. Vacuoles of leaf and root cells are acidified by V-ATPase and PPase proton pumps resulting in a slightly acidic vacuolar lumen (pH ~6) and a rather modest ΔpH. This is also the case in petunia leaves. Here, we show that vacuoles in epidermal petal cells are more acidic and are hyperacidified by a distinct proton-pumping system consisting of a P_{3A}-ATPase (PH5) and a P_{3B}-ATPase (PH1) that both reside in the tonoplast and directly interact with each other. The role of PH1 and PH5 in vacuolar acidification is supported by several findings.

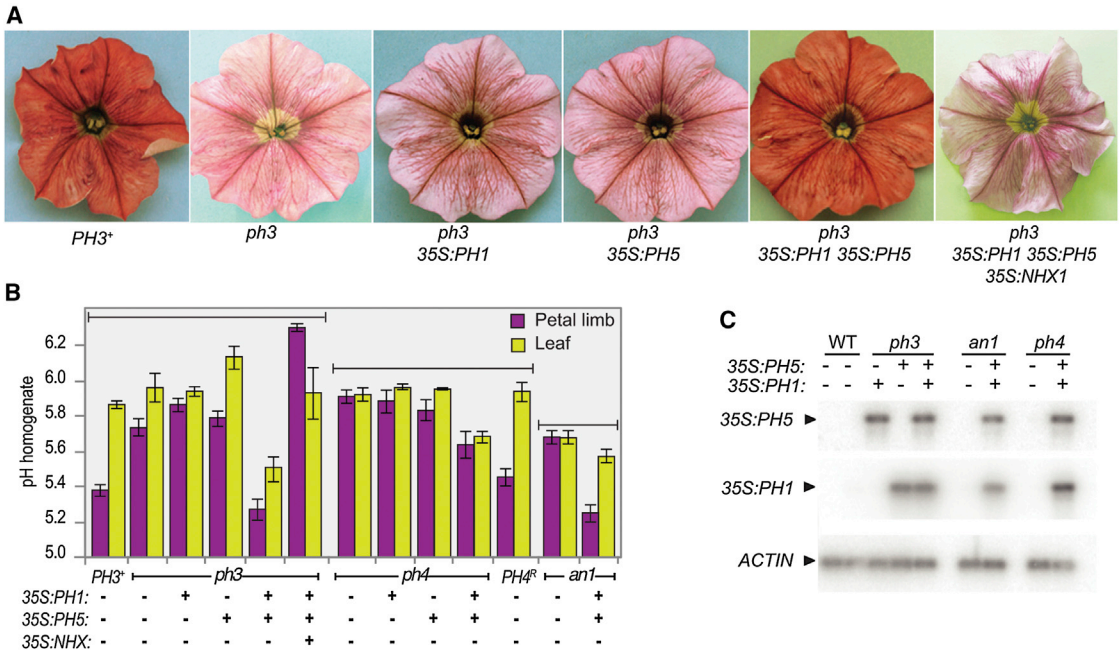

Figure 5. Constitutive Expression of PH1 and PH5 Restores Vacuolar Acidification in *ph3*, *ph4*, and *an1* Mutants

(A and B) Phenotypes and pH (mean ± SD; n ≥ 3) of petal and leaf extracts from *PH3*$^+$, *ph3* mutants and transgenic *ph3* siblings expressing *35S:PH1*, *35S:PH5* and/or *35S:NHX1*. Bracketed lines indicate genotypes grown and analyzed simultaneously.

(C) RT-PCR analysis of *35S:PH1* and *35S:PH5* transgenes in the plants shown in (A) and (B).

First, mutations that inactivate PH1, PH5, or transcription factors required for their expression (AN1, PH3, PH4) reduce the acidity of vacuoles in petals. Moreover, constitutive expression of the H^+ exchanger NHX phenocopies loss of function *ph* mutants, indicating that their blue flower colors and the increased pH of petal extracts are consequences of reduced vacuolar acidity. It is important to note that the vacuolar pH measured by nuclear magnetic resonance (NMR) is an average for epidermal and mesophyll cells and consequently underestimates the hyperacidification of vacuoles by *PH* genes, which is confined to (adaxial) epidermal cells (Quattrocchio et al., 2006; Verweij et al., 2008). In transgenic *35S:PH1 35S:PH5* plants, PH1 and PH5 are constitutively expressed in virtually all cells. The 35S promoter is, although active in all cells, considerably weaker than the endogenous promoters (Quattrocchio et al., 2013), resulting in a relatively small vacuolar pH shift.

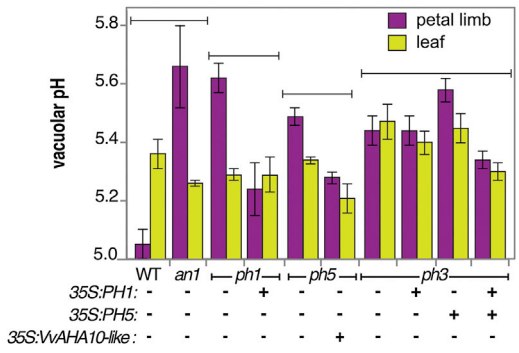

Figure 6. Vacuolar pH in Leaves and Petals of Different Mutants

Vacuolar pH (mean ± SE; n = 3) in leaves and petals of different genotypes as measured by ^{31}P-NMR. Bracketed lines indicate genotypes grown and analyzed within the same experiment. See also Figure S4.

Second, genetic data show that PH1 and PH5 are necessary and also sufficient to hyperacidify vacuoles in *ph3* petals and, when ectopically expressed, in leaves. PH3, PH4, AN1, and AN11 jointly activate the expression of *PH1*, *PH5*, and an unknown number (greater than ten) of additional genes, These downstream genes might encode proteins that enhance proton import into the vacuole directly (e.g., by activating PH5) or indirectly (by dissipating $\Delta\psi$). Furthermore, PH3 and PH4 might repress the expression of transporters mediating a proton efflux from the vacuole (e.g., H^+ antiporters, like NHX). Given that expression of *PH1* and *PH5* (transgenes) is sufficient to rescue the vacuolar pH defects in *ph3* petals, we conclude that these are the major, if not only, AN1/PH3/PH4-regulated genes that are involved in vacuolar acidification. Although we cannot exclude that some of the other target genes have a modest role in vacuolar acidification, they are more likely to function in other AN1/PH3/PH4-regulated processes, like, for example, the stabilization of anthocyanins in the vacuole (Quattrocchio et al., 2006).

Third, the bulk of PH1-GFPi expressed in stable transformants resides in the tonoplast, similar to PH5-GFP (Verweij et al., 2008). This indicates that both proteins directly mediate ion transport across the tonoplast, consistent with electrophysiological data

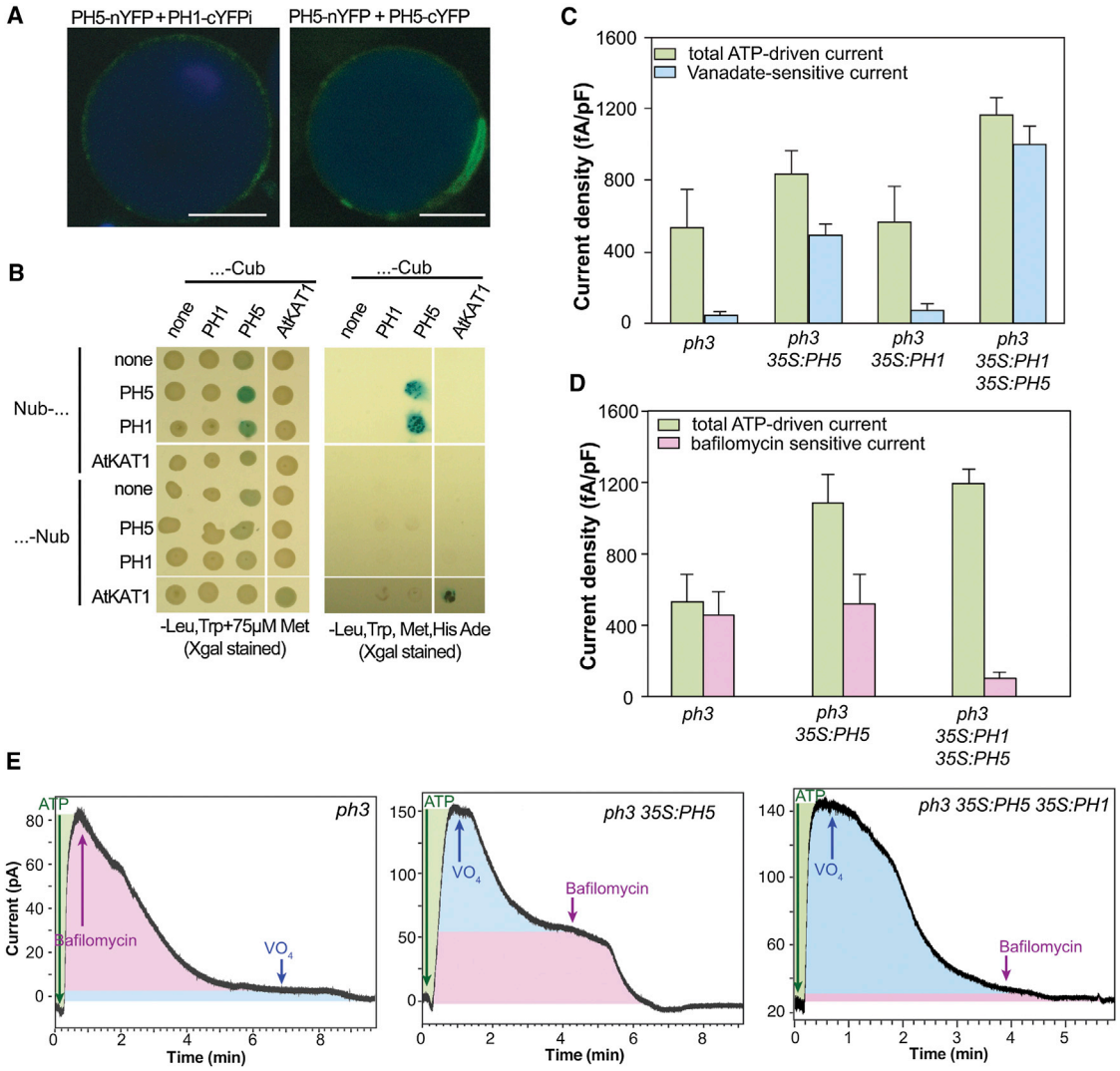

Figure 7. Interaction between PH1 and PH5

(A) Bimolecular fluorescence complementation by transient expression of PH5-nYFP and PH1-cYFP$_i$ or PH5-cYFP in epidermal petal protoplasts. YFP fluorescence is seen in green, autofluorescence of anthocyanins in blue.

(B) Split-ubiquitin yeast two-hybrid assays. Fusions of the C-terminal (Cub) and N-terminal ubiquitin moiety (Nub) were coexpressed in yeast and assayed for LacZ activity (blue staining) or growth on media lacking histidine (HIS) and adenine (ADE). AtKAT1 homodimerization (Obrdlik et al., 2004) is the positive control.

(C and D) (C) Vanadate-sensitive and total ATP-driven currents (mean ± SE, n ≥ 11) in the vacuolar membrane of leaf cells of the indicated genotypes and in (D) bafilomycin-sensitive and total ATP-driven currents (mean ± SE, n ≥ 4). All currents were measured in the whole-vacuole patch clamp, with membrane voltage clamped at 0 mV (±SE).

(E) ATP-driven vanadate-sensitive and bafilomycin-sensitive currents in leaf vacuoles from different genotypes. Green arrows, start of 5 mM Mg-ATP perfusion; blue arrow, switch to perfusion with 5 mM MgATP and 100 μM vanadate; magenta arrow, switch to perfusion with 5 mM MgATP and 40 nM bafilomycin. Sign convention for endomembranes was applied. Total ATP-driven currents, vanadate-sensitive currents, and bafilomycin-sensitive currents are indicated by green, blue, and magenta shading of the areas under the curves. Blue arrow: switch to perfusion with 5 mM MgATP and 100 μM vanadate. Magenta arrow, switch to perfusion with 5 mM MgATP and 40 nM bafilomycin.

See also Figures S5 and S6.

on patch-clamped vacuoles. We cannot exclude that minor amounts of PH1-GFPi localize to puncta in the cytoplasm, which may mark intermediate compartments like Golgi, vesicles, or prevacuoles through which PH1 reaches the tonoplast. Hence, PH1 and PH5 may also contribute to the acidification of these compartments in conjunction with specific V-ATPase isoforms residing there (Krebs et al., 2010).

Fourth, PH1 and PH5 interact in vivo as shown by yeast Split Ubiquitin Y2H assay and BiFC experiments in petal protoplasts. Plasma membrane P_{3A}-ATPases form homodimers and autoinhibit their partners via a C-terminal regulatory domain (R). In plants autoinhibition is overcome by phosphorylation (Fuglsang et al., 1999, 2007; Svennelid et al., 1999) and formation of an active P-ATPase hexamer bound to six 14-3-3 proteins

(Kanczewska et al., 2005; Ottmann et al., 2007), and/or by binding to RIN4, a regulator of plant immunity (Liu et al., 2009). P_{3A}-ATPases of fungi (*Neurospora*) also exist as dimers or hexamers, but hexamerization does not involve 14-3-3 proteins and the hexamers are thought to be a reservoir of inactive protein (Kühlbrandt, 2004). Our results unveil yet another way to regulate P_{3A}-ATPase activity, by interaction with an unrelated P-ATPase.

In the absence of PH1, PH5 can form homodimers and mediate an ATP-driven current across the tonoplast, which suffices to (partially) rescue a yeast P_{3A}-ATPase mutant and facilitate tannin accumulation in the seed coat. PH5 and the *Arabidopsis* homolog AHA10 (Baxter et al., 2005) are presumably needed to generate the pH gradient that drives the vacuolar import of (precursors of) tannins via the H^+ exchanger TT12 (Marinova et al., 2007). Although PH1 is coexpressed with PH5 in developing petunia seeds, it is not essential for tannin accumulation, and AHA10 drives tannin accumulation in the absence of PH1, as a PH1 homolog is missing in *Arabidopsis*. In the petal epidermis, however, PH1 is essential to hyperacidify vacuoles. Although PH1 does not sustain a detectable current in patch-clamped leaf vacuoles on its own, it roughly doubles the PH5-mediated current. This effect of PH1 is independent from a role in dissipating the voltage ($\Delta\psi$) across the tonoplast, because that was clamped at 0 mV in our experiments, and instead suggests that binding of PH1 to PH5 directly enhances the rate of proton pumping. If *ph1* were to reduce PH5 activity in vivo by only 50%, one would expect *ph1* petals to be more acidic than *ph5* petals, which is not the case. Possibly the PH1 dependency of PH5, whereas only 50% at 0 mV, increases with the rising $\Delta\psi$, which would make PH1 essential to generate the large ΔpH found in vivo. Furthermore, PH1 might contribute to vacuolar acidification in more than one way.

The high similarity with bacterial MgtA/MgtB suggests that PH1 may translocate Mg^{2+} (or other cations) from the vacuolar lumen into the cytoplasm. Such an activity could help to dissipate the voltage ($\Delta\psi$) built by proton pumping, and/or to create a local cation spike in the immediate vicinity of PH5, which favors 14-3-3 binding to release autoinhibition (Chevalier et al., 2009). However, PH1 could not replace the Mg^{2+} transporters ALR1 and ALR2 in yeast, which might be caused by the absence of certain proteins or misfolding and localization of PH1 in yeast. We consider the latter option unlikely because in yeast PH5 is (partially) active and PH5-CUB interacts with PH1-NUB. It is noteworthy that Mg^{2+} transport from the vacuole (plants) or periplasm (bacteria) to the cytoplasm does not require energy, raising the question why an ATP-driven pump would be involved. This, together with redundancy Mg transporters, suggests that the prime activity of MgtA might be the transport of another compound that remains to be discovered (Kehres and Maguire, 2002). Hence, PH1 may translocate a different ion or boost PH5 activity in an entirely different way.

Why do some specific tissues use two P-ATPases instead of the ubiquitous V-ATPase to acidify their vacuoles? V-ATPases transport four (at low ΔpH) to two (at high ΔpH) protons per ATP hydrolyzed (Rienmüller et al., 2012). P_{3A}-ATPases on the other hand transport only one proton per ATP hydrolyzed, and backflow of protons is prevented by conformational changes of the protein during proton translocation (Palmgren and Nissen, 2011) enabling them to pump against a larger electrochemical gradient. The V-ATPase pumping rate is limited by the electrochemical gradient ($\Delta\mu^{H+}$) and consequently decreases if other proton pumps are active (Rea and Sanders, 1987). Given that $\Delta\mu^{H+}$ was clamped at zero in our patch-clamp experiments, the observed reduction of the vanadate-resistant/bafilomycin-sensitive currents in vacuoles from leaf cells expressing PH1 and PH5 seems due to a (unknown) mechanism that is not reversed in the experimental setting. One possibility is a that the decreased vacuolar pH caused by PH1/PH5 activity triggers the disassembly of the V-ATPase complex, as seen in yeast and animal cells (Kane, 2012; Sze et al., 1999), or other structural changes (Schnitzer et al., 2011). Although it remains unclear how PH1 and PH5 downregulate V-ATPase activity, this indicates that vacuolar (hyper)acidification in PH1–PH5-expressing leaves almost entirely relies on these P-ATPases.

The most obvious function of the PH1–PH5 system is the modification of petal color, which may explain why the regulation of *PH1* and *PH5* is linked to that of anthocyanin genes through a partially overlapping set of transcription factors. This function seems conserved in distantly related species, as inactivation of the PH4 homolog in soybean also results in blue flowers and reduced acidity of cell extracts (Takahashi et al., 2013). Petal color is important for the attraction of pollinators and, hence, reproduction (Hoballah et al., 2007), which might explain why plants that are pollinated in other ways and have uncolored flowers, like *Arabidopsis*, do not have a *PH1* gene. Vacuolar hyperacidification by the PH1–PH5 system is probably not limited to flowers. *Nicotiana* expresses the PH5 homolog PMA9 in stem conductive tissues, in meristematic cells of axillary buds and adventitious roots, but the function of PMA9 in these tissues is unknown (Oufattole et al., 2000).

Further analysis of complexes of PH5, PH1, and other proteins (14-3-3) may provide insights on P-ATPase activation and how closely related P_{3A}-ATPases diverged in function and regulation. Altering *PH1* and *PH5* expression may provide a strategy for eliciting large changes in vacuolar pH (much larger than by altering expression of PPase or certain V-ATPase subunits) in order to enhance the transport of other ions, like Na^+ or K^+ via secondary transporters, such as the NHX antiporter, for research and applied purposes.

EXPERIMENTAL PROCEDURES

Genetic Stocks

All plants were grown under normal greenhouse conditions except where stated otherwise. The lines W225 ($an1^{W225}$), W134 ($an1^{W134}$), R144 ($ph3^{V2068}$), R150 ($ph4^{V2153}$), R160 ($ph2^{A2414}$), and R159 ($ph5^{R159}$) contain recessive alleles in the background of the "wild type" line R27. Lines V23, V38, V48, and R67 harbor stable recessive *ph1* alleles in unrelated backgrounds. The F1 hybrids R143 ($ph3^{R143}$) × R144, V64 ($ph4^{V64}$) × R150, and W242 ($an1^{W242}$) × W225 were used as transformable *ph3*, *ph4*, and *an1* mutants. Transformable *ph1* mutants were F1 hybrid R67 × V23 or *ph1* progeny selected from the F_2 cross V30 (*PH1*) × V23 (*ph1*). Protoplasts were from the F_1 hybrid M1 × V30 (full wild-type). The *an1 35S:AN1-GR* line and conditions for dexamethasone and/or cycloheximide treatments were described before (Spelt et al., 2000).

Expression Analyses

RT-PCR analysis of *PH5*, *DFR*, *GAPDH*, and *ACTIN* was carried out as described (Quattrocchio et al., 2006; Verweij et al., 2008). For RT-PCR of

PH1, we used primers #4001 (CACCATGTGGTTATCCAATATTTTCCCTGT) and #4023 (CAAGCATGATGCTGATAAGCAC), for *35S:PH5* #54 (CACTAGT GATATCACAAGTTTGTACA) and #1812 (GAATCAATGTAAGTGATTGCAG-TCCG), and for *35S:PH1* #54 and #4023 (CAAGCATGATGCTGATAAGCAC). RT-PCR products were amplified using a reduced number of cycles (*GAPDH*, *ACTIN*, *DFR*, *35S:PH1*, and *35S:PH5*, 20 cycles; *PH5*, 25 cycles; *PH1* 30 cycles) and visualized by DNA gel-blot analysis (Quattrocchio et al., 2006; Verweij et al., 2008).

Real-time PCR analysis was done with a Eco Real time PCR system (Illumina) using the SensiMix (Bioline QT650-05) following instructions of the producer. For *ACTIN* mRNA we used primers #5922 (TGCACTCCCACATGC TATCCT) and #5923 (TCAGCCGAAGTGGTGAAAGAG), for *DFR* #4900 (ACC TATGGATTTCGAGTCCAAAGA) and #4901 (CACATGATTCAAT GATGCTTA GCAT), for *PH1* #5932 (CTTGTTCAAAAACCCAGTGGACA) and #5934 (TCAGTTCTCGACCCTCCATC), and for *PH5* #5641 (TAGCAATCCTAAATGAT GGCACT) and #5642 (CAACTATCAGGTCTTGGAGATGG).

Immunoblot analysis was done as described (Verweij et al., 2008). Developmental stages of flowers were defined as follows: stage 1–2, young buds; 3–4, nearly fully expanded bud; 5–6, open(ing) flowers.

Phylogenetic Analysis

The tree was constructed from a ClustalW alignment of the full size protein sequences and a web-based version of the PHYLIP algorithm for maximum likelihood (PhyML, http://phylogeny.fr/version2_cgi/simple_phylogeny.cgi/). The proteins in the tree from the 3B and 2C clades represent the first result coming from BLAST search in the different species when the petunia PH1 protein was used as query. The proteins in the PH5 clade are the first results from BLAST search with the petunia PH5 protein as query. Other P3A ATPases were chosen in order to show the differences within the 3A clade.

Construction of Transgenes for Expression in Plant Cells

The PH1 coding sequence was amplified from genomic DNA using Phusion polymerase (Finnzymes) and primers complementary to start (#4001 CAC CATGTGGTTATCCAATATTTTCCCTGT) and stop codon (#3917 TAGGAC TAAAGCCATGTCTTGAA), cloned in pENTR/D-TOPO (Invitrogen), and recombined into the pB7WG2.0 expression vector (*35S:PH1*) or into pK7WGF2 (*35S:GFP-PH1*). To generate *35S:PH1-GFP*, a genomic *PH1* fragment, amplified with primers #4001 and #4002 (AAGCCATGTCTTGAATACCAAAATG), was cloned into pENTR/D-TOPO and recombined into pK7FWG2. The *MgtA* coding sequence was amplified with primers #4621 (ATACCATGTTATGTT TAAAGAAATTTTTACCCGGTTCA) and #4622 (ATAGCGGCCGCATGAA CAAAGCTCACTTTGTCTG), digested with NcoI/NotI, ligated in pENTR4, and recombined in the vector pK2GW7 (*35S:MgtA*), or pK7WGF2 (*p35S:GFP-MgtA*). *PH1:GFPi* was generated by triple-fusion PCR using (1) a *PH1* cDNA fragment from line V30 (codons 1–194) amplified with primers #5491 (GGG GACAAGTTTGTACAAAAAA-GCAGGCTCAATGTGGTTACCCAATATTT) and #5586 (GCATGGACGAGCTGTACAA-GATTGTTCAAACTGAGGTACAGGTT), (2) the GFP coding sequence amplified with #5584 (AGGTTCAAAGATGTG CAGGTAGAATGGTGAGCAAGGGCGAGGA) and #5585 (AACCTGTACCTC AGTTTGAACAATCTTGTACAGCTCGTCCATGC), and (3) a genomic *PH1* fragment from V30 containing the remainder of the coding sequence amplified with primers #5586 (GCATGGACGAGCTGTACAAGATTGTTCAAA-CTGAGGTA CAGGTT) and #5492 (GGGGACCACTTTGTACAAGAAAGCTGGGTAG-GACT AAAGCCATGTCTTGA). The three PCR products were mixed and reamplified with external primers (#5491 and #5492) to yield a single PCR product, which was recombined with BP clonase in pDONR P1-P2 (Invitrogen) and subsequently recombined into the pK2GW7 vector. *35S:PH1-cYFP*^{i} was made in a similar way using (1) a PH1 cDNA fragment amplified with primers #5491 and #5704 (GTCGGCGAGCTGCACGCTGCCTCTACCTGCACATCTTTGA ACCT), (2) cYFP amplified with #5705 (AGGTTCAAAGATGTGCAGGTAGAGG CAGCGTGCAGCTCG-CCGAC) and #5585 (AACCTGTACCTCAGTTTGAAC AATCTTGTACAGCTC-GTCCATGC), and (3) a genomic *PH1* fragment amplified with primers #5586 (GCATGGACGAGCTGTACAAGATTGTTCAAACT GAGG TACAGGTT) and #5492. The combined amplification product was then digested with BglII and NotI, inserted between the BamHI and NotI sites of pENTR4 (Invitrogen) and subsequently recombined into pK2GW7. The *35S:PH5-nYFP* and *35S:PH5-cYFP* constructs were obtained by recombining the pENTR clone containing the entire genomic fragment of *PH5* (from start to stop codon) into the nYFP/pUGW2 and cYFP/pUGW2 expression vectors respectively. See the Supplemental Experimental Procedures for details on gene constructs and plasmids used for heterologous complementation.

Split Ubiquitin Assay

Constructs expressing fusions of PH1 and PH5 to the C-terminal domain of ubiquitin (Cub) or a mutated form of the N-terminal domain (NubG) were generated and assayed for interaction in yeast as described (Obrdlik et al., 2004).

Protoplast Isolation, Transformation and Confocal Microscopy

Protoplast isolation and transient transformation was done as described (Faraco et al., 2011). GFP was imaged with a LSM Pascal Zeiss or a Bio-Rad 2000 confocal microscope.

pH Measurements

The pH of crude petal and leaf extracts was measured as described (Verweij et al., 2008).

^{31}P-NMR spectra were recorded on a standard broadband 10 mm probe (AMX 600 spectrometer, Bruker Analytische Messtechnik) with TopSpin version 1.3 software. The recording was done at 242.9 MHz without lock, with a Waltz-based broadband proton decoupling and a spectral window of 16 kHz. Chemical shifts were measured relative to the signal from a glass capillary containing 33 mM methylene diphosphonate (MDP), which is at 18.5 ppm relative to the signal from 85% H_3PO_4. In vivo ^{31}P-NMR experiments were carried out packing four flower limbs, or three leaves into a 10 mm diameter NMR tube with a perfusion system in which medium (1 mM MES-BTP [pH 6.1], 0.4 mM $CaSO_4$) was aerated, thermoregulated (25°C), and flowed at 10 ml min^{-1}. Resonances assignment was obtained as described (Kime et al., 1982; Roberts et al., 1980). Vacuolar pH was estimated from the chemical shift (δ) of inorganic phosphate (Pi) resonance. A titration curve was constructed from the δ of 2.5 mM KH_2PO_4 dissolved in 25 mM KCl, 20 mM $MgSO_4$, 5 mM citrate acid, 5 mM malic acid buffered in the pH range from 5 to 6.5 with 10 mM MES-KOH to obtain a ionic strength similar to the cell sap of the petal limbs.

pH values of crude tissue homogenates can vary due to environmental condition, though differences between genotypes are constant. For direct comparison, different genotypes were measured within one experiment. Given that NMR spectroscopy is time consuming, and in order to minimize effects of variable environmental conditions plants used for NMR analysis were therefore maintained in a growth chamber.

Patch-Clamp Recordings of Vacuolar Pump Currents

Protoplasts were isolated from petunia leaves, and vacuoles were patch clamped as previously described (van den Wijngaard et al., 2001). Currents are depicted following the convention for electrical measurements on endomembranes (Bertl et al., 1992). The current amplitude (fA) of a single vacuole was normalized against the membrane capacity (pF) of the vacuole to compensate for size differences between vacuoles. Vanadate-sensitive and bafilomycin-sensitive currents of seven to nine vacuoles from each genotype were averaged and plotted ±SE.

ACCESSION NUMBERS

The GenBank accession numbers for the *PH1* mRNA, gene, and protein sequences reported in this paper are KF690733 and KF690732.

SUPPLEMENTAL INFORMATION

Supplemental Information includes Supplemental Experimental Procedures and six figures and can be found with this article online at http://dx.doi.org/10.1016/j.celrep.2013.12.009.

AUTHORS CONTRIBUTIONS

R.K., L.E., and F.M.Q. conceived and designed the experiments; M.F., C.S., M.B., W.V., A.H., L.E., B.P., E.T., R.J., G.-P.D.S., R.K., and F.M.Q. performed

the experiments; M.F., C.S., L.E., A.H.d.B., G.-P.D.S., R.K., and F.M.Q. analyzed the data; and M.F., L.E., R.K., and F.M.Q. wrote the paper.

ACKNOWLEDGMENTS

We thank Ronald Breedijk, Erik Manders, Linda Joosen, Dorus Gadella, and colleagues (Center for Advanced Microscopy, Section Molecular Cytology, Swammerdam Institute for Life Sciences, University of Amsterdam) for use of microscopy facilities and technical assistance; Pieter Hoogeveen, Martina Meesters, and Daisy Kloos for plant care; and Michael Maguire (Case Western Reserve University) and Richard Gardner (University of Auckland) for materials and advice on the yeast and bacterial mutants. We are grateful to the two anonymous reviewers for helpful suggestions and comments. This work was supported by a grant (VGC.6717) from the Netherlands Technology Foundation with aid from Netherlands Organization for the Advancement of Research (NWO) (to R.K. and F.M.Q.), a short-term EMBO fellowship (to M.F.), a Visitors Travel Grant of NWO (to A.H.), and the project Reti di Laboratori Pubblici di Ricerca per la Selezione, Caratterizzazione e Conservazione di Germoplasma 2009 (to G.-P.D.S.).

Received: March 15, 2013
Revised: October 14, 2013
Accepted: December 4, 2013
Published: January 2, 2014

REFERENCES

Assaad, F.F., Qiu, J.L., Youngs, H., Ehrhardt, D., Zimmerli, L., Kalde, M., Wanner, G., Peck, S.C., Edwards, H., Ramonell, K., et al. (2004). The PEN1 syntaxin defines a novel cellular compartment upon fungal attack and is required for the timely assembly of papillae. Mol. Biol. Cell *15*, 5118–5129.

Barbier-Brygoo, H., De Angeli, A., Filleur, S., Frachisse, J.M., Gambale, F., Thomine, S., and Wege, S. (2011). Anion channels/transporters in plants: from molecular bases to regulatory networks. Annu. Rev. Plant Biol. *62*, 25–51.

Bassil, E., Tajima, H., Liang, Y.C., Ohto, M.A., Ushijima, K., Nakano, R., Esumi, T., Coku, A., Belmonte, M., and Blumwald, E. (2011). The Arabidopsis Na+/H+ antiporters NHX1 and NHX2 control vacuolar pH and K+ homeostasis to regulate growth, flower development, and reproduction. Plant Cell *23*, 3482–3497.

Baxter, I.R., Young, J.C., Armstrong, G., Foster, N., Bogenschutz, N., Cordova, T., Peer, W.A., Hazen, S.P., Murphy, A.S., and Harper, J.F. (2005). A plasma membrane H+-ATPase is required for the formation of proanthocyanidins in the seed coat endothelium of Arabidopsis thaliana. Proc. Natl. Acad. Sci. USA *102*, 2649–2654.

Bertl, A., Blumwald, E., Coronado, R., Eisenberg, R., Findlay, G., Gradmann, D., Hille, B., Köhler, K., Kolb, H.A., MacRobbie, E., et al. (1992). Electrical measurements on endomembranes. Science *258*, 873–874.

Casey, J.R., Grinstein, S., and Orlowski, J. (2010). Sensors and regulators of intracellular pH. Nat. Rev. Mol. Cell Biol. *11*, 50–61.

Chevalier, D., Morris, E.R., and Walker, J.C. (2009). 14-3-3 and FHA domains mediate phosphoprotein interactions. Annu. Rev. Plant Biol. *60*, 67–91.

de Vlaming, P., Schram, A.W., and Wiering, H. (1983). Genes affecting flower colour and pH of flower limb homogenates in *Petunia hybrida*. Theor. Appl. Genet. *66*, 271–278.

Faraco, M., Di Sansebastiano, G.P., Spelt, K., Koes, R.E., and Quattrocchio, F.M. (2011). One protoplast is not the other!. Plant Physiol. *156*, 474–478.

Fuglsang, A.T., Visconti, S., Drumm, K., Jahn, T., Stensballe, A., Mattei, B., Jensen, O.N., Aducci, P., and Palmgren, M.G. (1999). Binding of 14-3-3 protein to the plasma membrane H(+)-ATPase AHA2 involves the three C-terminal residues Tyr(946)-Thr-Val and requires phosphorylation of Thr(947). J. Biol. Chem. *274*, 36774–36780.

Fuglsang, A.T., Guo, Y., Cuin, T.A., Qiu, Q., Song, C., Kristiansen, K.A., Bych, K., Schulz, A., Shabala, S., Schumaker, K.S., et al. (2007). Arabidopsis protein kinase PKS5 inhibits the plasma membrane H+ -ATPase by preventing interaction with 14-3-3 protein. Plant Cell *19*, 1617–1634.

Fukada-Tanaka, S., Inagaki, Y., Yamaguchi, T., Saito, N., and Iida, S. (2000). Colour-enhancing protein in blue petals. Nature *407*, 581.

Gaxiola, R.A., Palmgren, M.G., and Schumacher, K. (2007). Plant proton pumps. FEBS Lett. *581*, 2204–2214.

Goodman, C.D., Casati, P., and Walbot, V. (2004). A multidrug resistance-associated protein involved in anthocyanin transport in *Zea mays*. Plant Cell *16*, 1812–1826.

Graves, A.R., Curran, P.K., Smith, C.L., and Mindell, J.A. (2008). The Cl^-/H^+ antiporter ClC-7 is the primary chloride permeation pathway in lysosomes. Nature *453*, 788–792.

Hoballah, M.E., Gübitz, T., Stuurman, J., Broger, L., Barone, M., Mandel, T., Dell'Olivo, A., Arnold, M., and Kuhlemeier, C. (2007). Single gene-mediated shift in pollinator attraction in Petunia. Plant Cell *19*, 779–790.

Kanczewska, J., Marco, S., Vandermeeren, C., Maudoux, O., Rigaud, J.L., and Boutry, M. (2005). Activation of the plant plasma membrane H+-ATPase by phosphorylation and binding of 14-3-3 proteins converts a dimer into a hexamer. Proc. Natl. Acad. Sci. USA *102*, 11675–11680.

Kane, P.M. (2012). Targeting reversible disassembly as a mechanism of controlling V-ATPase activity. Curr. Protein Pept. Sci. *13*, 117–123.

Kehres, D.G., and Maguire, M.E. (2002). Structure, properties and regulation of magnesium transport proteins. Biometals *15*, 261–270.

Kime, M.J., Ratcliffe, R.G., Williams, R.J.P., and Loughman, B. (1982). The application of ^{31}P nuclear magnetic resonance to higher plant tissue. I. Detection of spectra. J. Exp. Bot. *33*, 656–669.

Koes, R., Verweij, W., and Quattrocchio, F. (2005). Flavonoids: a colorful model for the regulation and evolution of biochemical pathways. Trends Plant Sci. *10*, 236–242.

Krebs, M., Beyhl, D., Görlich, E., Al-Rasheid, K.A.S., Marten, I., Stierhof, Y.D., Hedrich, R., and Schumacher, K. (2010). Arabidopsis V-ATPase activity at the tonoplast is required for efficient nutrient storage but not for sodium accumulation. Proc. Natl. Acad. Sci. USA *107*, 3251–3256.

Kühlbrandt, W. (2004). Biology, structure and mechanism of P-type ATPases. Nat. Rev. Mol. Cell Biol. *5*, 282–295.

Li, L., Tutone, A.F., Drummond, R.S.M., Gardner, R.C., and Luan, S. (2001). A novel family of magnesium transport genes in Arabidopsis. Plant Cell *13*, 2761–2775.

Liu, J., Elmore, J.M., Fuglsang, A.T., Palmgren, M.G., Staskawicz, B.J., and Coaker, G. (2009). RIN4 functions with plasma membrane H^+-ATPases to regulate stomatal apertures during pathogen attack. PLoS Biol. *7*, e1000139.

Maeshima, M. (2001). TONOPLAST TRANSPORTERS: Organization and Function. Annu. Rev. Plant Physiol. Plant Mol. Biol. *52*, 469–497.

Maguire, M.E. (2006). Magnesium transporters: properties, regulation and structure. Front. Biosci. *11*, 3149–3163.

Marinova, K., Pourcel, L., Weder, B., Schwarz, M., Barron, D., Routaboul, J.M., Debeaujon, I., and Klein, M. (2007). The Arabidopsis MATE transporter TT12 acts as a vacuolar flavonoid/H^+ -antiporter active in proanthocyanidin-accumulating cells of the seed coat. Plant Cell *19*, 2023–2038.

Marty, F. (1999). Plant vacuoles. Plant Cell *11*, 587–600.

Mindell, J.A. (2012). Lysosomal acidification mechanisms. Annu. Rev. Physiol. *74*, 69–86.

Obrdlik, P., El-Bakkoury, M., Hamacher, T., Cappellaro, C., Vilarino, C., Fleischer, C., Ellerbrok, H., Kamuzinzi, R., Ledent, V., Blaudez, D., et al. (2004). K^+ channel interactions detected by a genetic system optimized for systematic studies of membrane protein interactions. Proc. Natl. Acad. Sci. USA *101*, 12242–12247.

Ottmann, C., Marco, S., Jaspert, N., Marcon, C., Schauer, N., Weyand, M., Vandermeeren, C., Duby, G., Boutry, M., Wittinghofer, A., et al. (2007). Structure of a 14-3-3 coordinated hexamer of the plant plasma membrane H^+ -ATPase by combining X-ray crystallography and electron cryomicroscopy. Mol. Cell *25*, 427–440.

Oufattole, M., Arango, M., and Boutry, M. (2000). Identification and expression of three new Nicotiana plumbaginifolia genes which encode isoforms of a

plasma-membrane H(+)-ATPase, and one of which is induced by mechanical stress. Planta *210*, 715–722.

Palmgren, M.G., and Nissen, P. (2011). P-type ATPases. Annu. Rev. Biophys. *40*, 243–266.

Pedersen, C.N., Axelsen, K.B., Harper, J.F., and Palmgren, M.G. (2012). Evolution of plant p-type ATPases. Front. Plant Sci. *3*, 31.

Quattrocchio, F., Verweij, W., Kroon, A., Spelt, C., Mol, J., and Koes, R. (2006). PH4 of Petunia is an R2R3 MYB protein that activates vacuolar acidification through interactions with basic-helix-loop-helix transcription factors of the anthocyanin pathway. Plant Cell *18*, 1274–1291.

Quattrocchio, F.M., Spelt, C., and Koes, R. (2013). Transgenes and protein localization: myths and legends. Trends Plant Sci. *18*, 473–476.

Rea, P.A., and Sanders, D. (1987). Tonoplast energization: Two H^+ pumps, one membrane. Physiol. Plant. *71*, 131–141.

Rienmüller, F., Dreyer, I., Schönknecht, G., Schulz, A., Schumacher, K., Nagy, R., Martinoia, E., Marten, I., and Hedrich, R. (2012). Luminal and cytosolic pH feedback on proton pump activity and ATP affinity of V-type ATPase from Arabidopsis. J. Biol. Chem. *287*, 8986–8993.

Roberts, J.K.M. (1987). NMR in plant biochemistry. In The Biochemistry of Plants, Vol 13: Methodology, D.D. Davies, ed. (London: Academic Press), pp. 181–227.

Roberts, J.K.M., Ray, P.M., Wade Jardetzky, N., and Jardetzky, O. (1980). Estimation of cytoplasmic and vacuolar pH in higher plant cells by ^{31}P-NMR. Nature *283*, 870–872.

Schnitzer, D., Seidel, T., Sander, T., Golldack, D., and Dietz, K.J. (2011). The cellular energization state affects peripheral stalk stability of plant vacuolar H+-ATPase and impairs vacuolar acidification. Plant Cell Physiol. *52*, 946–956.

Smith, D.L., Tao, T., and Maguire, M.E. (1993). Membrane topology of a P-type ATPase. The MgtB magnesium transport protein of Salmonella typhimurium. J. Biol. Chem. *268*, 22469–22479.

Spelt, C., Quattrocchio, F., Mol, J.N., and Koes, R. (2000). anthocyanin1 of petunia encodes a basic helix-loop-helix protein that directly activates transcription of structural anthocyanin genes. Plant Cell *12*, 1619–1632.

Spelt, C., Quattrocchio, F., Mol, J., and Koes, R. (2002). *ANTHOCYANIN1* of petunia controls pigment synthesis, vacuolar pH, and seed coat development by genetically distinct mechanisms. Plant Cell *14*, 2121–2135.

Svennelid, F., Olsson, A., Piotrowski, M., Rosenquist, M., Ottman, C., Larsson, C., Oecking, C., and Sommarin, M. (1999). Phosphorylation of Thr-948 at the C terminus of the plasma membrane H(+)-ATPase creates a binding site for the regulatory 14-3-3 protein. Plant Cell *11*, 2379–2391.

Sze, H. (1985). H^+-Translocating ATPases: Advances using membrane vesicles. Annu. Rev. Plant Physiol. *36*, 175–208.

Sze, H., Li, X., and Palmgren, M.G. (1999). Energization of plant cell membranes by H+-pumping ATPases. Regulation and biosynthesis. Plant Cell *11*, 677–690.

Takahashi, R., Yamagishi, N., and Yoshikawa, N. (2013). A MYB Transcription Factor Controls Flower Color in Soybean. J. Hered. *104*, 149–153.

Thever, M.D., and Saier, M.H., Jr. (2009). Bioinformatic characterization of p-type ATPases encoded within the fully sequenced genomes of 26 eukaryotes. J. Membr. Biol. *229*, 115–130.

van den Wijngaard, P.W., Bunney, T.D., Roobeek, I., Schönknecht, G., and de Boer, A.H. (2001). Slow vacuolar channels from barley mesophyll cells are regulated by 14-3-3 proteins. FEBS Lett. *488*, 100–104.

van Houwelingen, A., Souer, E., Mol, J.N.M., and Koes, R.E. (1999). Epigenetic interactions among three dTph1 transposons in two homologous chromosomes activate a new excision-repair mechanism in petunia. Plant Cell *11*, 1319–1336.

Verweij, C.W. (2007). Vacuolar acidification: Mechanism, regulation and function in petunia flowers (Amsterdam: VU-University).

Verweij, W., Spelt, C., Di Sansebastiano, G.P., Vermeer, J., Reale, L., Ferranti, F., Koes, R., and Quattrocchio, F. (2008). An H^+ P-ATPase on the tonoplast determines vacuolar pH and flower colour. Nat. Cell Biol. *10*, 1456–1462.

Yamaguchi, T., Fukada-Tanaka, S., Inagaki, Y., Saito, N., Yonekura-Sakakibara, K., Tanaka, Y., Kusumi, T., and Iida, S. (2001). Genes encoding the vacuolar Na^+/H^+ exchanger and flower coloration. Plant Cell Physiol. *42*, 451–461.

Yoshida, K., Kondo, T., Okazaki, Y., and Katou, K. (1995). Cause of blue petal colour. Nature *373*, 291.

Yoshida, K., Mori, M., and Kondo, T. (2009). Blue flower color development by anthocyanins: from chemical structure to cell physiology. Nat. Prod. Rep. *26*, 884–915.